ACS Macro Letters

Letter

pubs.acs.org/macroletters

# Programmable Liquid Crystal Elastomers Prepared by Thiol–Ene Photopolymerization

Taylor H. Ware,[†,‡,§] Zachary P. Perry,[‡,∥] Claire M. Middleton,[‡,§] Scott T. Iacono,[∥] and Timothy J. White*[,‡]

[‡]Materials and Manufacturing Directorate, Air Force Research Laboratory, Wright-Patterson Air Force Base, Ohio 45433, United States

[§]Azimuth Corporation, Beavercreek, Ohio 45431, United States

[∥]Department of Chemistry and Chemistry Research Center, United States Air Force Academy, Colorado Springs, Colorado 80840, United States

Supporting Information

**ABSTRACT:** The spontaneous conversion of a flat film into a 3-D shape requires local programming of the mechanical response. Historically, the ability to locally program the mechanical response of high strain (>30%) liquid crystalline elastomers (LCEs) has been limited to magnetic or mechanical alignment techniques, which limits spatial resolution. Recently, we reported on the preparation of LCEs capable of 55% strain with spatial control of the mechanical response at scales as small as 0.01 mm$^2$. Here, we report a distinct formulation strategy to realize programmable stimulus-response in LCEs. Photopolymerization of thiol–ene/acrylate formulations yields materials that exhibit large reversible strain up to 150%. The photopolymerization reaction is extremely rapid, reducing preparation time from days to minutes. The mechanical behavior of these materials can be tuned by varying cross-link density. Spatial and hierarchical programming of the director profile is demonstrated, enabling 3-D shape change, including twisting ribbons and localized Gaussian curvature.

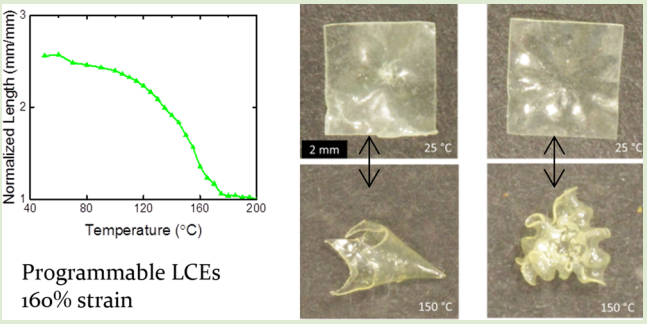


Materials capable of reversibly changing shape have the potential to enable simple mechanical devices, where traditional mechanical elements are difficult to employ.[1] Such materials are often categorized by the magnitude and complexity of achievable shape change in response to a given stimulus. Through patterning, it has been demonstrated that hydrogels, semicrystalline polymers, and liquid crystal networks can be designed to undergo complex shape change in response to solvents, light, and heat.[2−4] Complex shape change in monolithic materials is achieved through spatial and hierarchical control of the magnitude or direction of stimuli-response. In ordered materials this can be achieved through spatial control of molecular orientation.

The polymerization of liquid crystalline monomers can retain the order within an elastic solid.[5] In uniaxially aligned liquid crystalline elastomers (LCEs), lightly cross-linked networks, reversible strains greater than 300% have been reported.[6] Oriented LCEs have typically been aligned by mechanical loading or magnetic fields, which can generate films with uniaxial or relatively simple patterns.[7,8] In densely cross-linked liquid crystal polymers, surface alignment techniques, such as rubbing or photoalignment, have been employed to prepare ordered polymer networks with comparatively complex local alignment.[9] Recently, main-chain LCEs that are amenable to photoalignment have been demonstrated, allowing for arbitrary spatial alignment of the nematic director over regions as small as 0.01 mm$^2$.[10] Key to the realization of this material was the use of a two-step synthesis, comprised of the Michael addition of a nematic diacrylate to a primary amine followed by subsequent cross-linking of the telechelic diacrylate oligomer, which results in a LCE that exhibits maximum strains of 55%.[11] Critically, this reaction scheme can proceed in one-pot (a liquid crystal cell), exhibits a wide nematic phase window, and proceeds without the addition of solvent.

The set of reactions between thiols and alkenes has received considerable attention in the field of responsive polymers.[12] In particular, the radical polymerization of thiols with a wide variety of alkenes has been noted for well-defined networks and efficient reaction in the bulk. Several recent examples of systems of thiol–ene-based LCEs have been described.[13−17] These materials chemistries enable facile processing of mechanically aligned LCEs and high-strain microactuators, but a synthetic avenue to surface-alignable thiol–ene LCEs has not been reported to our knowledge. In this work, we describe a thiol–ene/acrylate formulation strategy to prepare LCEs in a

**Received:** July 23, 2015
**Accepted:** August 10, 2015
**Published:** August 17, 2015




DOI: 10.1021/acsmacrolett.5b00511
*ACS Macro Lett.* 2015, 4, 942−946

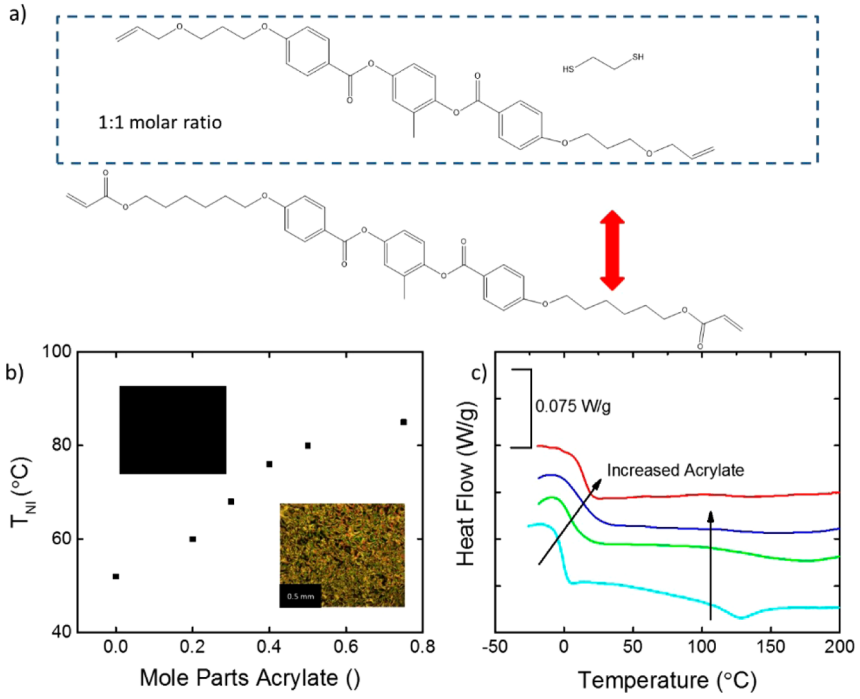


**Figure 1.** (a) Chemical structures of the thiol (EDT), alkene (RM2AE), and acrylate (RM82) monomers. (b) Each of the compositions examined here exhibit a nematic phase above room temperature. The nematic−isotropic transition temperature, as determined by polarized optical microscopy (upper inset, isotropic phase; lower inset, nematic phase) of the monomer depends on the acrylate composition. (c) After polymerization, the materials exhibit glass transition temperatures below room temperature and a nematic−isotropic transition. Compositions shown are 0.3 RM82, 0.4 RM82, 0.5 RM82, and 0.75 RM82.

one-step radical polymerization. Like our recent report,[10] this chemistry is also sensitive to surface alignment, allowing for facile spatial programming of the local director orientation of the LCEs.

Surface-alignable LCEs have several unique formulation and preparation requirements. A primary difficulty in formulating the materials chemistry is ensuring that liquid crystallinity is maintained when nonmesogenic monomers are added. The phase behavior of the monomer solution is largely controlled by the weight fraction of the individual components. As such, in step-growth reactions, such as the radical polymerization of thiols and alkenes, it is critical to limit the molecular weight per functionality of nonmesogenic monomers. This was illustrated in our initial formulation attempts not detailed here primarily focused on mixtures employing multifunctional thiols commonly used in thiol−ene polymerizations, such as pentaerythritol tetrakis(3-mercaptopropionate), which has a molecular weight per thiol of 122 g/mol. These formulations did not exhibit the required combination of a readily alignable nematic phase that could be polymerized into an aligned LCE. As such we sought to minimize the fraction of nonmesogenic monomer through the use of 1,2-ethanedithiol (EDT), which has a molecular weight per thiol of 47 g/mol. The formulation strategy that we employ here is illustrated in Figure 1a. A mesogenic diallyl ether, 2-methyl-1,4-phenylene bis(4-(3-(allyloxy)propoxy)benzoate) (RM2AE) and EDT are mixed with a 1:1 molar ratio. The radical photopolymerization of these monomers produces a linear liquid crystalline polymer. Thus, cross-links are introduced with the inclusion of the nematic diacrylate monomer, 1,4-bis-[4-(6-acryloyloxyhexyloxy)benzoyloxy]-2-methylbenzene (RM82). Accordingly, the formulations examined here have a stoichiometric excess of alkenes. RM82 can participate in both the thiol−ene reaction and homopolymerize, which may lead to unreacted allyl groups.[12] The mesomorphic phase behavior of the monomer mixtures is shown in Figure 1b with inset polarized optical micrographs that confirm a Schlieren texture is apparent below the nematic to isotropic transition temperature ($T_{NI}$) and the mixtures exhibit no residual birefringence after melting to an isotropic liquid. The acrylate concentration is indicated in mole parts when added to one mole part of RM2AE and 1 mol part EDT. Differential scanning calorimetry (Figure 1c) was used to isolate the thermal behavior of the polymers. Each composition reported here exhibits a glass transition temperature ($T_g$) below room temperature and compositions with low acrylate content exhibit a nematic to isotropic transition above 100 °C. Both the $T_g$ and the $T_{NI}$ increase with acrylate content. As the acrylate content increases, the enthalpy of the order−disorder transition decreases in magnitude. As confirmed by polarized optical microscopy, compositions with less than 0.4 mol parts RM82 completely transition to an isotropic state, while higher acrylate compositions retain some birefringence at high temperatures. This indicates that the materials retain a paranematic state previously reported in some LCEs.[18] As is evident in Table 1, the gel fraction of the formulations increases with acrylate concentration, despite possible competing factors such as unreacted allyl groups. The composition and gel fraction of each material tested is summarized in Table 1.

Each of these monomer systems can be aligned in a liquid crystal cell with treated surfaces, such as rubbed polymer surfaces or photoalignment layers. Polarized optical micrographs of a representative (0.5 RM82) composition after alignment and polymerization in a liquid crystal cell with antiparallel rubbed surfaces is shown in Figure 2a. The polymer is largely free of defects and exhibits the expected birefringence



DOI: 10.1021/acsmacrolett.5b00511
*ACS Macro Lett.* 2015, 4, 942−946

**Table 1. Molar Compositions and Gel Fraction of Liquid Crystal Elastomers**

| RM82 | RM2AE | EDT | gel fraction (g/g) |
|---|---|---|---|
| 0.75 | 1 | 1 | 0.86 ± 0.02 |
| 0.5 | 1 | 1 | 0.76 ± 0.02 |
| 0.4 | 1 | 1 | 0.72 ± 0.01 |
| 0.3 | 1 | 1 | 0.69 ± 0.03 |
| 0.2 | 1 | 1 | 0.50 ± 0.02 |
| 0 | 1 | 1 | 0 |

of a uniaxially aligned LCE. This alignment was confirmed with wide-angle X-ray scattering (Figure 2b). It should be noted that, while the order is derived from surface anchoring, the order and orientation of the molecules propagates through the thickness of the material. At $2\theta = 20°$, scattering expected from a material exhibiting the nematic phase is evident in the azimuthal integration of scattering intensity (Figure 2c). This aligned film also exhibits anisotropic modulus when subjected to uniaxial tensile loading (Figure 2d). Along the director, loading produces an elastic response and failure below 50% strain. When the material is loaded perpendicular to the director, a highly nonlinear mechanical response is observed (commonly referred to as "soft elasticity"). Specifically, as evident in Figure 2d, the material in this orientation initially is elastic and then becomes nonlinear exhibiting a broad stress plateau to continued stretch. It should be noted that here we plot engineering stress and strain, and that inhomogeneous deformation is observed (necking), as has been reported for some other LCEs.[19]

In response to a change in temperature, all of the compositions exhibited reversible change in shape. Polarized optical micrographs of 0.5 RM82 at room temperature and at 200 °C are shown in Figure 3a. Although not shown, the material completely returns to the original dimensions on cooling to room temperature. The shape change evident in Figure 3a is the result of a large contraction along the rubbing direction coupled with perpendicular expansion in the plane and through the thickness. The magnitude of the strain is dependent on the concentration of diacrylate. The maximum reversible strain (measured on cooling) is 156%, for the LCE prepared with a molar concentration of 0.4 RM82. This is nearly 3× larger than our recent study of surface alignable LCEs.[10] As acrylate concentration increases, the achievable reversible strain decreases (Figure 3b). Interestingly, as acrylate concentration decreases from 0.4 reversible strain also decreases. As the gel fractions (Table 1) indicate, this decrease in reversible strain may be due to low network strength limited by the relatively low cross-link density and low gel fraction.

The through-thickness (hierarchical) orientation of liquid crystal polymers can be used to generate bending and torsional deflections.[20] Hierarchical variation is prohibitively difficult to achieve by mechanical or magnetic fields. Because of the ability to use surfaces to align the materials compositions reported here, the twisted nematic orientation where the director varies 90° through the thickness can be readily prepared. As with recent reports, offsetting the nematic director to the long axis of the sample by 30° (Figure S1) produces torsional deformations. On heating, the sample morphs from flat to a twisted conformation until the film is limited by self-intersection (Figure 3c). Nearly 300° of twist per millimeter of material is achievable (Figure 3d). As a point of reference, this is larger than high performance torsional carbon nanotube yarns, although direct comparison between these materials systems requires caution.[21] The director profile can also be programmed in-plane, to prepare films subsumed with topological defects. Topological defects describe point discontinuities in ordered media. In LCEs, topological defects have been proposed as a mathematical way to describe director patterns that can be used to design complex LCE shape changing materials.[22] In this work, we chose two patterns, namely, a +1 azimuthal defect and a +6 defect. The strength of the defect reflects the number of 360° changes of the director orientation observed when traveling around the defect center. The +1 azimuthal defect (Figure S2) was predicted theoretically and then confirmed to produce a point of

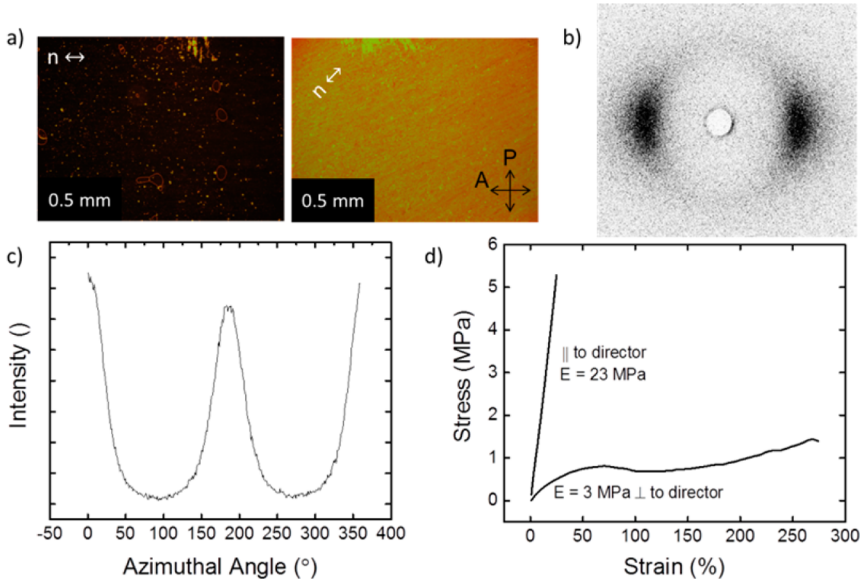


**Figure 2.** (a) Polarized optical micrographs of an aligned LCE (0.5 RM82) at 0° and 45° to the polarizer. (b, c) Wide-angle X-ray scattering shows anisotropic scattering indicative of a material in the nematic phase. The 2D scattering profile (b) and azimuthal integration (c) of the wide angle scattering are shown. (d) Uniaxial tensile testing indicates anisotropic mechanical properties and so-called "soft elasticity".



DOI: 10.1021/acsmacrolett.5b00511
*ACS Macro Lett.* 2015, 4, 942−946

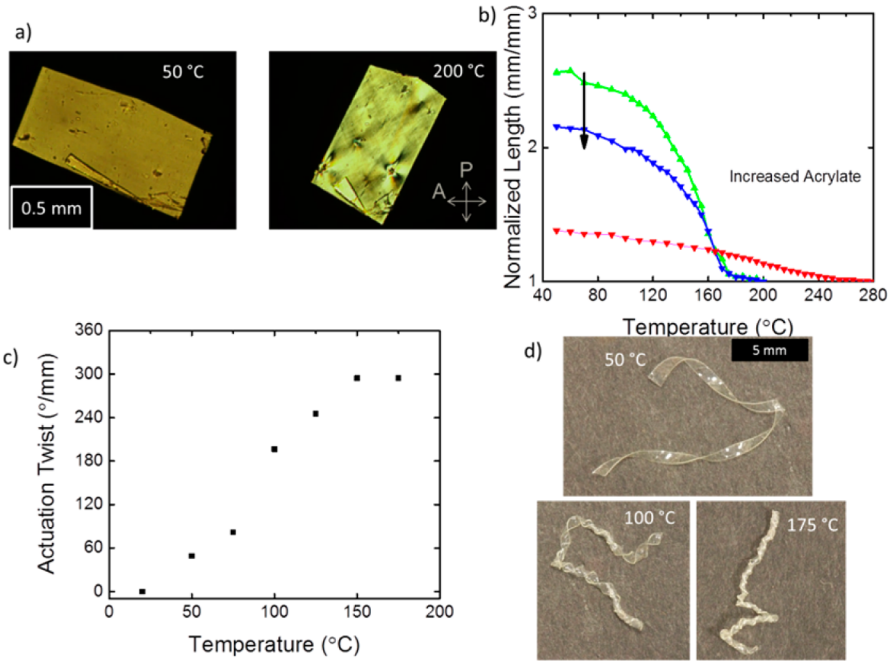


**Figure 3.** (a) Polarized optical micrographs of a representative LCE (0.5 RM82) at room temperature and 200 °C. (b) Quantitative measurement of the reversible shape change of three compositions (0.4RM82−0.75RM82). (c) Twisted nematic alignment can be used to induce torsional shape change which increases as a function of temperature. (d) Representative photographs of the twisted nematic film with varying twist. All data were collected on cooling.

Gaussian curvature and, as such, change from a flat film to a cone on exposure to an order-reducing stimulus such as heat.[23,24] Here a 50 $\mu$m thick flat film morphs to a cone more than 5 mm tall with a sharp opening angle of 39° at 150 °C (Figure 4a,b; Supporting Information, Video). The +6 defect forms a 2D wrinkling pattern that leads to an areal contraction (Figure 4c,d). Both of these films return to a largely flat state on cooling (pictures taken after three actuation cycles) although some residual stress is retained. Complete reversibility of the flat state is an intense focus of our ongoing research. Each of these director patterns utilizes the large reversible strain and surface alignable nature of the materials formulation reported here to generate complex deformation of the thiol−ene LCE. It is expected that this chemistry could be readily adopted to achieve many distinct shape changes through further design of the director profile. In closing, the thiol−ene/acrylate formulation described here is a facile approach to generate high-strain, complexly programmed LCES through commercially available materials and a simple synthetic technique, namely, photopolymerization.

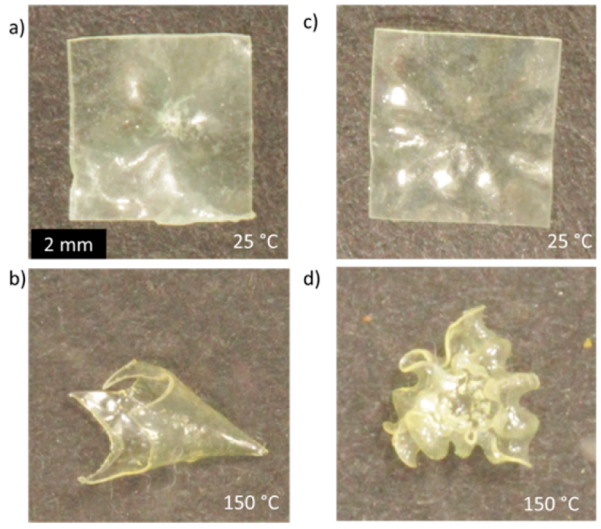


**Figure 4.** (a) Photograph of an LCE film with a subsumed +1 defect at room temperature and (b) upon heating to 150 °C. Note, in the photograph at 150 °C the material was rotated and laid on its side. (c) Photograph of an LCE film with a subsumed +6 defect. (d) Upon heating, the film transforms to a complex radial and azimuthal buckled structure. Photographs at room temperature were taken after three heating cycles.

## MATERIALS AND METHODS

RM82 (1,4-bis-[4-(6-acryloyloxyhexyloxy)benzoyloxy]-2-methylbenzene) was purchased from Synthon Chemicals. 1,2-Ethanedithiol (EDT) was purchased from Sigma-Aldrich. RM2AE (2-methyl-1,4-phenylene bis(4-(3-(allyloxy)propoxy)benzoate) was purchased from Alpha Micron. Irgacure 651 was donated by BASF. Elvamide was donated by DuPont. PAAD-22 was purchased from Beam Co. All materials were used as received unless otherwise noted.

Liquid crystal cells were prepared using methods described elsewhere.[10] Briefly for cells patterned using rubbed surfaces, Elvamide was dissolved in methanol at 0.15 wt %. This solution was then spin-coated on plasma-cleaned glass and then rubbed with a felt cloth to introduce alignment, either uniaxial or twisted. For photoaligned cells, PAAD-22 in dimethylformamide (0.33 wt %) and then spin coated on plasma-cleaned glass. The glass was then baked at 100 °C for 10 min. For either cell type, two pieces of glass were glued together using a two-part epoxy mixed with 50 $\mu$m glass spheres to set the cell thickness. After the cell was fabricated, photoalignment was carried out using a custom-built point-by-point irradiation system where the polarization of the light (445 nm) is used to orient the dye.

All formulations consisted of a 1:1 molar ratio of RM2AE and EDT. RM82 content was varied as indicated in Table 1. Irgacure 651 was used as a photoinitiator in concentrations of 0.1 wt %. While protecting the monomer mixture from fluorescent light, each



DOI: 10.1021/acsmacrolett.5b00511
ACS Macro Lett. 2015, 4, 942−946

monomer mixture was prepared in a vial, melted at ∼100 °C, and vortexed repeatedly. The phase behavior of the monomer solution was investigated using polarizing optical microscopy with a heating stage. The resulting nematic solution was then filled into a liquid crystal cell by capillary action at 100 °C, in the isotropic state. The cell was then cooled to 15 °C below $T_{NI}$ of the monomer and allowed to rest. This allows the nematic defects to relax and for the monomer to take the order dictated by the surface and polymerized using 365 nm UV light (∼200 mW/cm$^2$) at room temperature. Polymerization was carried out for 20 min, flipping the cell after 15 s and 10 min. Using a low intensity of UV light led to significant scattering in the sample.

Each film was characterized by a variety of methods. Gel fraction was determined by measuring the remaining mass of a film ∼10 mg in initial weight after immersion in acetone. Each composition was run in triplicate. Differential scanning calorimetry (TA Instruments Q1000) was used to investigate the thermal behavior of the system. Samples were heated in $N_2$ from room temperature to 150 °C, then cooled to −50 °C and heated to 200 °C. All heating and cooling rates were set to 10 °C/min. Data shown are of the second heating cycle. To facilitate data collection, samples 200 $\mu$m thick were prepared in cells without specific alignment dictated. $T_g$ is denoted as the midpoint of the transition. Shape change of uniaxially aligned samples was characterized by monitoring a rectangular sample ∼1 mm × ∼1 mm floating on a silicone bath. A thermal stage (top and bottom heating) was used to control temperature. All data were collected on cooling with temperature allowed to equilibrate for 5 min before recording an image (polarizing optical microscope) and sample size measured (ImageJ).

A single composition (0.5 RM82) was selected for further characterization. Wide angle X-ray scattering was used to measure alignment using a Rigaku Ultrax and Cu K$\alpha$ radiation on a sample with uniaxial alignment. Tensile testing was performed using a TA Instruments Q800. Samples were approximately 8 mm long by 2 mm wide and each orientation was run in triplicate. The strain rate was set to 100%/min. Torsional actuators were fabricated using Elvamide-coated glass rubbed in orthogonal directions. After polymerization the LCE was cut at 30° to a rubbing direction. The sample dimensions were 22 mm × 0.8 mm × 0.05 mm. Defect patterned samples were aligned using point-by-point photoalignment. Sample dimensions were 5 mm × 5 mm × 0.05 mm. For 3D shape change, ambient heating on a hot plate covered in black paper, as a nonadhesive surface, and inside a glass thermal chamber was used to monitor shape change.

## ■ ASSOCIATED CONTENT

### Supporting Information

Video of shape changing +1 defect; Schematics of director orientation. The Supporting Information is available free of charge on the ACS Publications website at DOI: 10.1021/acsmacrolett.5b00511.

(AVI)
(PDF)

## ■ AUTHOR INFORMATION

### Corresponding Author

*E-mail: timothy.white.24@us.af.mil.

### Present Address

†Department of Bioengineering, The University of Texas at Dallas, Dallas, Texas, United States.

### Notes

The authors declare no competing financial interest.

## ■ ACKNOWLEDGMENTS

T.H.W., C.M.M., and T.J.W. would like to acknowledge funding from the Materials and Manufacturing Directorate and the Office of Scientific Research of the Air Force Research Laboratory.

## ■ REFERENCES

(1) Mather, P. T.; Luo, X.; Rousseau, I. A. *Annu. Rev. Mater. Res.* **2009**, *39*, 445.
(2) Kim, J.; Hanna, J. A.; Byun, M.; Santangelo, C. D.; Hayward, R. C. *Science* **2012**, *335*, 1201.
(3) Turner, S. A.; Zhou, J.; Sheiko, S. S.; Ashby, V. S. *ACS Appl. Mater. Interfaces* **2014**, *6*, 8017.
(4) Ohm, C.; Brehmer, M.; Zentel, R. *Adv. Mater.* **2010**, *22*, 3366.
(5) Broer, D. J.; Finkelmann, H.; Kondo, K. *Makromol. Chem.* **1988**, *189*, 185.
(6) Wermter, H.; Finkelmann, H. *e-Polym.* **2001**, *013*, 1.
(7) Schuhladen, S.; Preller, F.; Rix, R.; Petsch, S.; Zentel, R.; Zappe, H. *Adv. Mater.* **2014**, *26*, 7247.
(8) Pei, Z.; Yang, Y.; Chen, Q.; Terentjev, E. M.; Wei, Y.; Ji, Y. *Nat. Mater.* **2013**, *13*, 36.
(9) Liu, D.; Broer, D. J. *Langmuir* **2014**, *30*, 13499.
(10) Ware, T. H.; McConney, M. E.; Wie, J. J.; Tondiglia, V. P.; White, T. J. *Science* **2015**, *347*, 982.
(11) Ware, T. H.; White, T. J. *Polym. Chem.* **2015**, *6*, 4835.
(12) Hoyle, C. E.; Bowman, C. N. *Angew. Chem., Int. Ed.* **2010**, *49*, 1540.
(13) Yang, H.; Buguin, A.; Taulemesse, J.-M.; Kaneko, K.; Méry, S.; Bergeret, A.; Keller, P. *J. Am. Chem. Soc.* **2009**, *131*, 15000.
(14) Yang, H.; Liu, M.-X.; Yao, Y.-W.; Tao, P.-Y.; Lin, B.-P.; Keller, P.; Zhang, X.-Q.; Sun, Y.; Guo, L.-X. *Macromolecules* **2013**, *46*, 3406.
(15) Yakacki, C. M.; Saed, M.; Nair, D. P.; Gong, T.; Reed, S. M.; Bowman, C. N. *RSC Adv.* **2015**, *5*, 18997.
(16) Fleischmann, E. K.; Forst, F. R.; Köder, K.; Kapernaum, N.; Zentel, R. *J. Mater. Chem. C* **2013**, *1*, 5885.
(17) Yang, H.; Buguin, A.; Taulemesse, J. M.; Kaneko, K.; Méry, S.; Bergeret, A.; Keller, P. *J. Am. Chem. Soc.* **2009**, *131*, 15000.
(18) Lebar, A.; Kutnjak, Z.; Žumer, S.; Finkelmann, H.; Sanchez-Ferrer, A.; Zalar, B. *Phys. Rev. Lett.* **2005**, *94*, 197801.
(19) Higaki, H.; Takigawa, T.; Urayama, K. *Macromolecules* **2013**, *46*, 5223.
(20) Lee, K. M.; Bunning, T. J.; White, T. J. *Adv. Mater.* **2012**, *24*, 2839.
(21) Lima, M. D.; Li, N.; de Andrade, M. J.; Fang, S.; Oh, J.; Spinks, G. M.; Kozlov, M. E.; Haines, C. S.; Suh, D.; Foroughi, J. *Science* **2012**, *338*, 928.
(22) Modes, C. D.; Warner, M. *Phys. Rev. E* **2011**, *84*, 021711/1.
(23) Modes, C. D.; Bhattacharya, K.; Warner, M. *Phys. Rev. E* **2010**, *81*, 060701.
(24) de Haan, L. T.; Schenning, A. P.; Broer, D. J. *Polymer* **2014**, *55*, 5885.



DOI: 10.1021/acsmacrolett.5b00511
*ACS Macro Lett.* 2015, 4, 942−946